LA-UR-13-26824
Approved for public release; distribution is unlimited.

Title: Formulation of the Constituent Distribution Model Implemented into the BISON Framework for the Analysis of Performance of Metallic Fuels with Some Initial Simulations Results

Author(s): Carlson, Neil N.
Unal, Cetin
Galloway, Jack D.

Intended for: AFC milestone report for M3FT-13LA0203121
Report

Issued: 2013-08-30

Formulation of the Constituent Distribution Model Implemented into the BISON Framework for the Analysis of Performance of Metallic Fuels with Some Initial Simulations Results

N. Carlson[1], C. Unal[2], J. Galloway[2]

Los Alamos National Laboratory

[1]Computer, Computational and Statistical Sciences Division
[2]Nuclear Engineering and Proliferation Division

An updated version of the paper presented at:
International Conference on Fast Reactors and Related Fuel Cycles: Safe Technologies and Sustainable Scenarios (FR13)
March 4-7 2013, Paris France

Abstract

This paper presents the progress of the fuel performance analysis using BISON [1] fuel performance tool. Within the BISON [1] framework a new Zirconium diffusion kernel was implemented that substantially improved the reliability and stability for solving Zirconium migration problems in metallic nuclear fuels. Several benchmark problems were created, including a simple 1-D rod and several 2-D segments of a fuel rod that covered several temperature regimes. The simulations were then compared to results from the code Pedernal [2], which is a "high-performance solver for coupled, nonlinear heat conduction and multi-component species diffusion". Comparison between the BISON [1] based solver and Pedernal showed exceptional agreement for all benchmark cases. Very small differences appeared at longer time frames (2,000 days) for the hotter fuel simulations; however this is believed to be due, primarily, to the different time-stepping algorithms used in the two codes. Overall the domain of the benchmark covered all components of the U-Pu-Zr phase diagram (alpha, delta, beta and gamma phases) and showed excellent agreement when compared to Pedernal based results.

1. INTRODUCTION

The prediction of fuel behavior under irradiation involves very complex material behavior. The understanding of fundamental mechanisms driving damage production and evolution is not at a desirable level of maturity and, in some cases, does not exist. To make advances toward to the development of predictive tools, it is clear that we need high-performance modeling and simulation (MS) techniques. The recent advances in computer hardware and simulation algorithms enable us now to simulate the atomistic and mesoscale behavior of materials, including radiation-induced damage at submicron scales, with the desired level of accuracy and computational efficiency.

It is also important to recognize that the fuel-clad interactions are primarily 3D in nature. The 1D capability of current models is not very useful for transients and local thermo-chemical interactions. Most material properties are affected by the microstructure characteristics of the materials. Predictions of transient behavior and fuel compressibility and fragmentation (especially for oxide fuels) will require microstructural-based swelling modeling approaches to account for the microchemical evolutions.

Current capabilities are focused on fuel pellets, although it is known that the limiting phenomenon could be associated with the behavior of the fuel assembly (assembly bowing, etc.). It is possible to design a fuel pellet for 40% burn-up, although this design may result in failures at much lower burn-ups because of 3D assembly distortions when it is placed in an assembly for many reasons. In addition, despite the fact that multiple computer codes are developed by many researchers, a robust predictive capability for quantifying fuel behavior and its uncertainty is still lacking. Large uncertainties and scatters still exist in the predictions, mainly because

- fuel rods are 3D structures, and large deformations may occur;
- fuel assemblies are 3D structures and can behave differently from a single fuel pellet;
- the constitutive materials laws are nonlinear as a result of creep, plasticity, and other material data;
- material behavior is anisotropic and time-dependent;
- material behavior is not fully understood;
- irradiation effects on materials is not a mature science and is not well understood;
- the fundamental data to verify materials modeling is lacking (in some cases, data cannot be taken directly, only indirectly);
- the physical process involved makes it difficult to define separate effects testing by controlling the boundary conditions to validate materials models;
- processes under irradiation conditions occur in a wide variety of time and length scales, each requiring different modeling techniques; and
- integrated multiscale, multiphysics modeling that covers all scales is lacking.

The most desirable approach in fuel modeling is to develop predictive tools with 3D capabilities because the location of fuel-cladding contact becomes critical for fuel-cladding chemical interactions. Some recent attempts have been made to create 3D codes with varying degrees of sophistication.

The primary objective of this work is to develop an initial capability using available models and the 3-D simulation code BISON [1] to analyze various experiments performed by Advanced Fuels Campaign (AFC). BISON is 3-D fuel performance analysis code being developed using the MOOSE [1] framework, a general purpose framework for the solution of differential equation. We have developed a pseudo-binary constituent migration model for U-Pu-Zr and implemented it into the BISON framework. We discuss preliminary results from an initial version of the model (we published this

part of the paper in Ref 11), and describe subsequent refinements to the model that have been made. Results from the later formulation will be presented in a companion paper. A basic ternary model of constituent migration has also been developed and is discussed.

2. CONSTITUENT REDISTRIBUTION MODEL

In this section we present a model [2] of constituent migration in a binary system that is based on the model developed in [3] for U-Zr nuclear fuel and later used in [4] in a pseudo-binary study of U-Pu-Zr fuel. A similar model is considered in [5]. These models adapt the original work of Shewmon [6] in the approach to 2-phase regions.
Consider a binary system consisting of components A and B. For simplicity we suppose that within some temperature range the system has a B-poor α phase and a B-rich β phase separated by a 2-phase $\alpha + \beta$ region . Letting c denote the concentration of B (B atoms per unit volume), we have the conservation law for B:

$$\frac{\partial c}{\partial t} + \nabla \cdot \mathbf{J} = 0, \tag{1}$$

where J is the flux of B atoms. A similar equation for the concentration of A atoms holds but with the opposite flux since we will assume that the net concentration of atoms remains uniform and constant. In a single-phase region we have

$$\mathbf{J} = -D_\pi \left(\nabla c + c \frac{Q_\pi^\star}{RT^2} \nabla T \right), \qquad \pi = \alpha \text{ or } \beta, \tag{2}$$

where T is the temperature, D_π is the diffusivity of B in phase π, Q_π^* is the heat of transport of B in phase π, and R is the gas constant. The last term involving ∇T is the so-called Soret effect or thermal diffusion. The coefficient Q_π^* may be either positive or negative. This term contributes an advective component to the B flux directed down the temperature gradient toward lower temperatures when positive, and up the temperature gradient toward higher temperatures when negative.

Next consider the 2-phase region very near the solubility limit of B in α. In this case the α phase predominates and we regard it as the connected matrix phase and the remaining B-rich β phase as the precipitant phase, which provides a reservoir of B atoms. The assumption now is that local equilibrium between α and β is maintained at each point in a temperature gradient through instantaneous adjustment of the phase fractions via rapid local diffusion processes. This means that c is constrained to lie on the solubility curve, which we will denote by c_α (T), and as a consequence $\nabla c = c'_\alpha(T) \nabla T$. Shewmon [6] instead employs a differential description of the curve

$$\frac{dc}{dT} = c \frac{\Delta H}{RT^2}, \tag{3}$$

where ΔH is a certain enthalpy of solution, from which ∇c can be expressed in terms of ∇T. The models developed in [4] and [5] adopt this viewpoint, but the expressions they use for ΔH are completely inconsistent with their phase diagrams, and even have the wrong sign in several cases. Thus for the sake of consistency, our model will adopt the

former approach where the solubility curves are given explicitly. If we further assume that the flux of B atoms occurs entirely through the matrix α phase, then we arrive at an expression for the flux J in the 2-phase region near the α solubility limit,

$$\mathbf{J} = -D_\alpha \left(c'_\alpha(T) + c_\alpha(T) \frac{Q^\star_\alpha}{RT^2} \right) \nabla T. \tag{4}$$

The analogous argument can be made for the flux in the 2-phase region near the solubility limit of A in β. There the flux is

$$\mathbf{J} = -D_\beta \left(c'_\beta(T) + c_\beta(T) \frac{Q^\star_\beta}{RT^2} \right) \nabla T, \tag{5}$$

where $c_\beta(T)$ is the corresponding solubility curve. The general flux in the 2-phase region is then defined to be the phase fraction weighted linear combination of (4) and (5):

$$\mathbf{J} = -\left[f_\alpha D_\alpha \left(c'_\alpha(T) + c_\alpha(T) \frac{Q^\star_\alpha}{RT^2} \right) + f_\beta D_\beta \left(c'_\beta(T) + c_\beta(T) \frac{Q^\star_\beta}{RT^2} \right) \right] \nabla T, \tag{6}$$

where $f_\alpha + f_\beta = 1$ and $f\alpha$ (c, T) is the phase fraction of α at temperature T and average composition c and is defined by the lever rule.

Two-Phase Implementation Of Species Distribution Model

The model we discussed above is very similar to the model of Kim et al. [4], but it differs in two significant ways. It corrects an inconsistency between the enthalpies of solution and the solubility limit curves of the phase diagram. It also adds an artificial diffusion term when in the 2-phase regime that stabilizes the standard Galerkin FE method used by BISON [1].

The Zr mass conservation equation takes the form

$$\frac{\partial C}{\partial t} = \nabla \cdot \mathcal{D} \nabla C + \nabla \cdot \mathcal{S} \nabla T \tag{7}$$

where C(x,t) is the Zr mole fraction, and $\mathcal{D}(T,C)$ and $\mathcal{S}$(T,C) are coefficients that depend on the temperature T(x, t) and the Zr mole fraction.

In a single-phase region of the phase diagram (here α denotes the arbitrary phase) we have the standard diffusion equation with

$$\mathcal{D}(T,C) = D_\alpha(T,C) \tag{8}$$

$$\mathcal{S}(T,C) = D_\alpha(T,C)\, C\, \frac{Q^\star_\alpha}{RT^2} \tag{9}$$

where Q^*_α is the heat of transport of Zr in the α phase.

In a 2-phase, α + β, region $C_\alpha(T) < C < C_\beta(T)$ bounded by the solubility limit curves C_α and C_β, the Soret term coefficient is

$$\mathcal{S}(T,C) = f_\alpha \mathcal{D}_\alpha(T, C_\alpha(T)) \left[\frac{dC_\alpha}{dT} + C_\alpha(T) \frac{Q^*_\alpha}{RT^2} \right] + (1 - f_\alpha) \mathcal{D}_\beta(T, C_\beta(T)) \left[\frac{dC_\beta}{dT} + C_\beta(T) \frac{Q^*_\beta}{RT^2} \right] \quad (10)$$

where

$$f_\alpha(T,C) = \frac{C_\beta(T) - C}{C_\beta(T) - C_\alpha(T)} \quad (11)$$

is the phase fraction of α according to the lever rule. In a 2-phase region one ought to take $\mathcal{D}(T,C) = 0$, however this would result in (8) becoming purely hyperbolic, and it is well-known that standard centered finite difference or Galerkin finite element schemes are unstable on such equations. Thus to stabilize the scheme used by BISON, we add a bit of artificial diffusion and take

$$\mathcal{D}(T,C) = f_\alpha D_\alpha(T, C_\alpha(T)) p_\alpha + (1 - f_\alpha) D_\beta(T, C_\beta(T)) p_\beta \quad (12)$$

where p_α and p_β are dimensionless numerical parameters taken as small as possible while maintaining stability.

Smoothing $\mathcal{D}$ and $\mathcal{S}$

As defined above, $\mathcal{D}$ and $\mathcal{S}$ do not vary smoothly (or even continuously) with (T,C) when crossing the phase diagram curves, and consequently the discretized system will be much more difficult to solve than it would otherwise be. We have ameliorated this effect by smoothing $\mathcal{D}$ and $\mathcal{S}$ in a small ε-neighborhood of the phase diagram curves.

First consider a time slab $T_a < T < T_b$ of the phase diagram corresponding to a 2-phase, $\alpha + \beta$, region. In the strip $[C_\alpha(T), C_\alpha(T) + \varepsilon_C]$ bordering the solubility curve C_α we take

$$\mathcal{D}(T,C) = g(s)\mathcal{D}_{\alpha+\beta}(T,C) + (1 - g(s))\mathcal{D}_\alpha(T,C), \quad \text{with } s \equiv \frac{C - C_\alpha(T)}{\epsilon_C} \quad (13)$$

where D_α and $D_{\alpha+\beta}$ denote the original diffusivities in the single and 2-phase regions defined in the previous section, and g is the smooth function $g(s) = s^2(3-2s)$. Similarly, in the strip $[C_\beta(T) - \varepsilon_C, C_\beta(T)]$ bordering the solubility curve C_β we take

$$\mathcal{D}(T,C) = g(s)\mathcal{D}_{\alpha+\beta}(T,C) + (1 - g(s))\mathcal{D}_\beta(T,C), \quad \text{with } s \equiv \frac{C_\beta(T) - C}{\epsilon_C} \quad (14)$$

Otherwise we do not modify $\mathcal{D}$. The Soret term coefficient $\mathcal{S}$ is smoothed in exactly the same way.

Next, when $|T - T_\alpha| < \varepsilon_T$ where the line $T = T_\alpha$ separates two time slabs of the phase diagram (e.g., α–δ and β–γ) we take

$$\mathcal{D}(T,C) = (1 - h(s))\mathcal{D}_1(T,C) + h(s)\mathcal{D}_2(T,C), \quad \text{with } s \equiv \frac{T - T_a}{\epsilon_T} \quad (15)$$

where $\mathcal{D}_1$ and $\mathcal{D}_2$ denote the smoothed diffusion coefficients computed in the time slab

below and above T = T_a as just described, and h is the smooth function h(s) = (1/4) (s + 1)^2(2 - s). Otherwise we do not modify the smoothed diffusion coefficient of a time slab. Again, S is smoothed in exactly the same way.

We apply the model described above to U-Zr and U-Pu-Zr nuclear fuel. In [4] it is argued that a pseudo-binary treatment of U-Pu-Zr, in which the Pu fraction is held fixed and uniform, is justified both theoretically and on the basis of experimental data which show that the Pu is largely immobile. We consider a fuel with a constant Pu content, and use the simple pseudo-binary phase diagram given in [4]. There are two different sets of 2-phase regions depending on the temperature range: $\alpha + \delta$, $\beta + \gamma$. The evolving Zr mole fraction distribution, c(x, t), is governed by the conservation law (1) with flux J given by (6) using diffusivities, heats of transport, and solubility limit curves corresponding to the local phases involved. In addition we solve for an evolving temperature field using the standard heat equation

$$\rho c_p \frac{\partial T}{\partial t} = \nabla \cdot k \nabla T + q(c,t) \qquad 16$$

with a variable heat source q that will depend on the local Zr fraction (actually the local fraction of actinides, which is the complement of the Zr fraction). This is a departure from the model studied in [4] which employed an adjusted fixed temperature profile. In this preliminary work, however, we used a constant, uniform internal heat generation, which will be modified in future work. In this work we compare our results with the Pedernal code, which also used a constant, uniform heat generation source for consistency. The phase properties used in this study are given in Table 1 and are those from [4]. For the remaining material properties that appear in the heat equation we use generic values for U-Zr found on the web: ρ= 19.05 g/cm^3, c_p = 0.3 J/g-K, k = 25.0 W/m-K.

Table. 1 Diffusion coefficients, D = D_0 exp(−Q/RT), and heats of transport for U-Pu-Zr phases.

Phase	α	δ	β	γ
D_0 (m^2/s)	3.0×10^{-6}	3.0×10^{-6}	1.14×10^{-5}	$10^{-5.1-8.05c+9.13c^2}$
Q (kJ/mol)	170	150	180	$128 - 107c + 174c^2$
Q^* (kJ/mol)	200	160	450	−200

3. RESULTS

Results generated using Bison are compared to identical problem definitions using the diffusion code called “Pedernal”, described in reference [2]. Several comparison problems were created and will be described. These comparison problems include a simple one-dimensional problem, and three two-dimensional problems pertaining to a quarter disk of a fuel rod where the three problems pertain to the bottom, middle and top of a representative rod with associated temperature distributions.

2-D Problems

Once acceptable agreement was achieved for the simple 1-D verification problem (not presented in this paper due to the page limit), with the problem domain encompassing the alpha and delta phases only, a more complex 2-D problem was used as a comparison case. As described in reference [1], this problem is based on the 4S Design 1 test problem studied in reference [4]. One of the U-Pu-Zr fuel designs studied in [4] was proposed for the conceptual 4S reactor. In design 1, the one we will consider here, the Zr content of the fuel is 22 at%, the fuel rod radius is 4.83 mm, and the fuel rod is subjected to a linear power of 19:7 kJ/m. In [4] several 1-D radial simulations were performed with different temperatures at the surface of the rod, reflecting the varying surface temperature along the length of the rod. For our 3-D test problem we will consider a rod of length 500 mm with an imposed surface temperature that varies linearly from 535 ^{o}C at the bottom (z = 0) to 605 ^{o}C at the top (z = 500 mm); these temperatures match the range of surface temperatures considered in [4]. The actual design length of the rod is 2.5 m, but even at 0.5 m the problem is essentially 1-D radial with no appreciable axial transport of heat or Zr. Using a shorter fuel rod allows the use of a somewhat smaller computational mesh with cells having a decent aspect ratio. At the ends of the rod we impose no heat flux, and impose no Zr flux on the entire outer surface of the rod. In this work we used a constant heat generation. Initially the Zr mole fraction is uniformly 0.22 and the temperature is at its quasi-steady state profile. In this study we used q(c) = constant in both the Bison and Pedernal simulations.

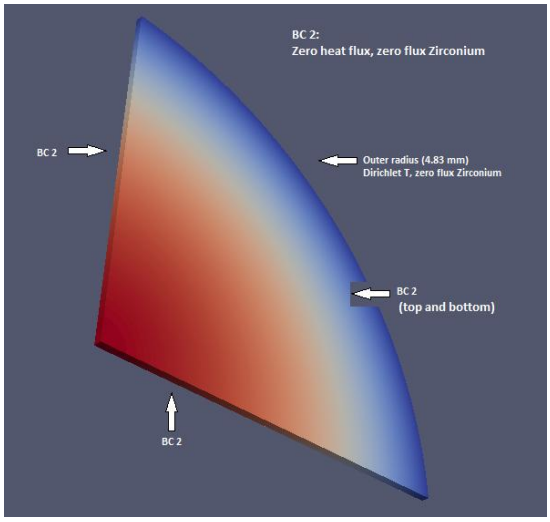

Figure 1: 2-D rod geometry and BCs.

In reference [2] three radial disks, ¼ symmetry of a rod, were simulated at three different axial heights which span all the four phases of the U-Pu-Zr phase diagram. Figure 1 shows the geometry layout along with the boundary conditions on all sides of the 2-D disk. The outer radius of the rod containing a dirichlet boundary in temperature and a zero flux Zirconium boundary condition, then all other boundaries (top, bottom, x=0, y=0) having zero heat flux, and zero flux Zirconium boundary conditions. A constant, uniform volumetric heat source was simulated, correlated with the stated linear heat

generation rate. Running this same problem geometry with Bison and Pedernal, results of Zirconium mole fraction versus rod radial distance were plotted as a function of time for both codes. The results for the rod bottom, rod middle and rod top are shown in Figures 2-4, respectively. In all three of these cases the agreement is excellent. At most times the results overlay so closely that delineation between the Bison line and the Pedernal line is hard to discern. Particularly, this is the case for all three results for the rod bottom simulation, where the only differences show up at the very rod outer edge, in the last mesh block. For Figure 3, rod middle, this trend still holds true up until the 2000 day simulation, whereupon a very small difference can be noticed near 0.031 meters, where the slop starts to ramp back up, this is the first central where line differentials are even noticed and the results are still in excellent agreement. Finally, the simulation for rod top, Figure 4, as in all cases shows excellent agreement; however a very small difference can be seen in the 2000 day simulation. It is believed the primary reason these small differences start to appear at longer simulation times is that the time step size used in Bison was not identical to that used in Pedernal. In fact, Pedernal has an automatic time stepping algorithm that adjusts the time step size on the fly according to convergence criteria, which will be discussed further in depth later.

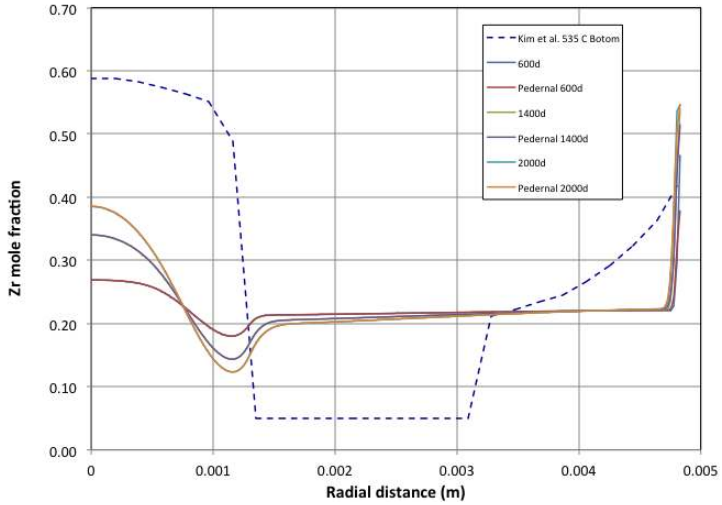

Figure 2: 2-D rod bottom, Bison-Pedernal comparison.

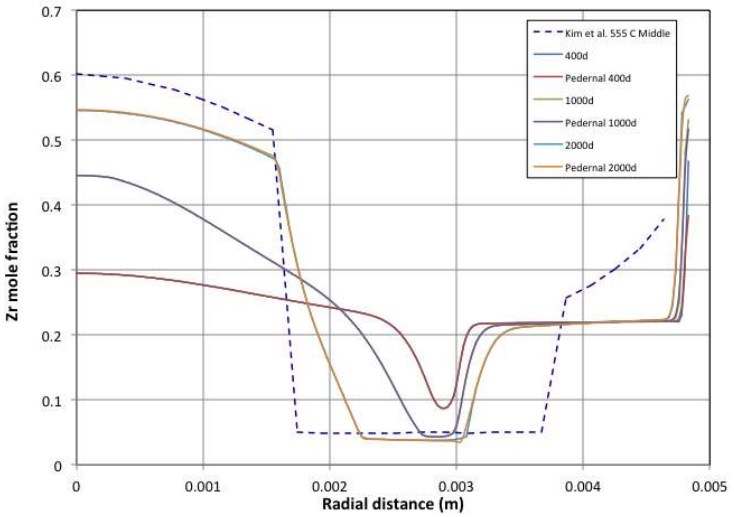

Figure 3: 2-D rod middle, Bison-Pedernal comparison.

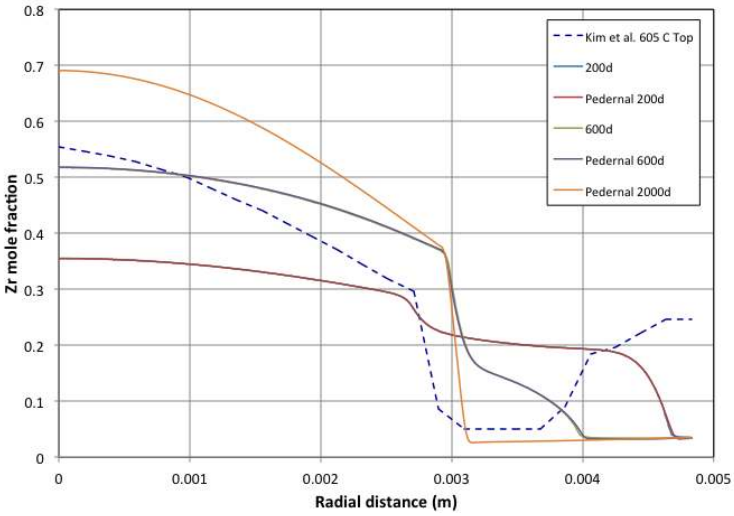

Figure 4: 2-D rod top, Bison-Pedernal comparison.

Figures 2-4 also show the results of Kim et al. (dashed blue lines). It is clear that there are some differences in the predicted zirconium profiles by BISON [1] using the constituent distribution model presented in this paper and Kim et al. [4]. These differences are primarily due to the temperature boundary conditions that are different in this study. We used a constant heat generation in the pellet and calculate the radial temperature profile that is quite different than the temperature profile used by Kim et al. The radial temperature profile used by Kim et al. was an adjusted temperature profile. In other words the adjusted radial temperature profile is used as a boundary conditions in their diffusion calculation. We plan to use a thermal conductivity model that depends upon temperature as well as zirconium concentration, and zirconium concentration dependent heat generation feature in the future work to account temperature-concentration-power-diffusion coupling correctly.

4. REVISED CONSTITUENT REDISTRIBUTION MODEL

Since obtaining the preceding results, we have made two improvements to the model. This section describes this revised U-Pu-Zr model, which is that currently implemented in Bison. It also has been validated against results from Pedernal.

First, to ensure a physical Zr mole fraction, $0 \le C \le 1 - C_{\mathrm{Pu}}$, where C_{Pu} is the fixed Pu mole fraction, it is necessary that the flux (2) tend to 0 as C tends to either limiting value. This is true for the lower limit, but not the upper limit. To address this issue we have inserted an additional factor into the Soret term coefficient, so that (9) becomes

$$S(T,C) = D_\alpha(T,C)\frac{C(1-C_{\mathrm{Pu}}-C)}{1-C_{\mathrm{Pu}}}\frac{Q_\alpha^\star}{RT^2}. \tag{17}$$

Second, we have restricted the form of solubility curves allowed in order to simplify the expression for the flux in two-phase regions. The original model allowed for any form of solubility curves $c_\alpha(T)$ and $c_\beta(T)$ (c.f. equations (4), (5), and (6)), although the implementation of the simplified U-Pu-Zr pseudo-binary phase diagram only used linear solubility curves. The revised model restricts to solubility curves $c(T)$ satisfying

$$\frac{dc}{dT} = \frac{c(1-C_{\mathrm{Pu}}-c)}{1-C_{\mathrm{Pu}}}\frac{\Delta H}{RT^2} \tag{18}$$

for some parameter ΔH. Solubility curves thus have the form

$$c(T) = (1-\mathrm{C_{Pu}})\left\{1+\frac{1-\mathrm{C_{Pu}}-c_0}{c_0}\exp\left[\frac{H}{R}\left(\frac{1}{T}-\frac{1}{T_0}\right)\right]\right\}^{-1}, \qquad c(T_0)=c_0, \tag{19}$$

for constants $c_0, T_0,$ and ΔH. As applied to the simplified U-Pu-Zr phase diagram, these curves are very nearly linear. With this and the first modification, the flux (4) becomes

$$\mathbf{J} = -D_\alpha\left(\frac{c_\alpha(T)(1-\mathrm{C_{Pu}}-c_\alpha(T))}{1-\mathrm{C_{Pu}}}\frac{\Delta H_\alpha + Q_\alpha^\star}{RT^2}\right)\nabla T. \tag{20}$$

The fluxes (5) and (6) are modified in the analogous manner. Consequently the two-phase Soret coefficient (10) becomes

$$\begin{aligned}\mathcal{S}(T,C) = {} & f_\alpha D_\alpha(T,C_\alpha(T))\left(\frac{C_\alpha(T)(1-C_{\mathrm{Pu}}-C_\alpha(T))}{1-C_{\mathrm{Pu}}}\frac{\Delta H_\alpha + Q_\alpha^\star}{RT^2}\right)+ \\ & (1-f_\alpha)D_\beta(T,C_\beta(T))\left(\frac{C_\beta(T)(1-C_{\mathrm{Pu}}-C_\beta(T))}{1-C_{\mathrm{Pu}}}\frac{\Delta H_\beta + Q_\beta^\star}{RT^2}\right)\end{aligned} \tag{21}$$

5. BASIC TERNARY MODEL

The preceding pseudo-binary model for U-Pu-Zr fuel was based on the observation that Pu does not appear to migrate significantly and thus could be ignored. Looking forward to more complex fuel types, such as U-Pu-Zr containing minor amounts of lanthanides or Pu-Am-Zr used in the FUTURIX-FTA test, there is a need to move beyond this binary

viewpoint and begin to investigate ternary models of constituent migration. To this end we have considered the following basic ternary model. This was derived using the procedure described in [7, Chapter 5].

Consider a ternary substitutional alloy with components A, B, and C, where component atoms diffuse via the vacancy mechanism. We make several simplifying assumptions. We assume a constant molar volume, independent of composition, and that the concentration of vacancies is very small and fixed at its equilibrium value. Let $c_A, c_B, c_C \geq 0$ be the component mole fractions, $c_A + c_B + c_C = 1$. In light of the last relation, one component can be eliminated. We will consider C to be the solvent and A and B to be solutes, and eliminate C. The fluxes for A and B are then

$$\begin{aligned} \mathbf{J}_A &= -\tilde{D}_{AA}\nabla c_A - \tilde{D}_{AB}\nabla c_B - \frac{c_A S_A}{RT^2}\nabla T \\ \mathbf{J}_B &= -\tilde{D}_{BA}\nabla c_A - \tilde{D}_{BB}\nabla c_B - \frac{c_B S_B}{RT^2}\nabla T \end{aligned} \tag{22}$$

where $\tilde{D}_{AA}, \tilde{D}_{AB}, \tilde{D}_{BA}$, and $\tilde{D}_{BB}$ are the interdiffusion coefficients of A and B relative to C, and S_A and S_B are Soret coefficients. All are functions of c_A and c_B; in particular the cross diffusivities $\tilde{D}_{AB}$ and $\tilde{D}_{BA}$ must tend to 0 as c_A and c_B, respectively, tend to either 0 or 1. The interdiffusion coefficients must further satisfy the conditions

$$\tilde{D}_{AA},\ \tilde{D}_{BB} > 0, \qquad \tilde{D}_{AA}\tilde{D}_{BB} > \tilde{D}_{AB}\tilde{D}_{BA} \geq 0. \tag{23}$$

This model, therefore, requires 6 material parameters as a function of temperature and composition, and that for each phase, compared to 2 material parameters for the binary model. Very little data is available on ternary interdiffusion coefficients for metal alloys. Petri and Dayananda [9] experimentally obtained the interdiffusion coefficients for U-Pu-Zr at a single composition (U-13Pu-12Zr) and temperature (1023K):

Interdiffusion coefficients relative to U ($10^{-12}\,\mathrm{m}^2/\mathrm{s}$)			
$\tilde{D}_{\mathrm{ZrZr}}$	$\tilde{D}_{\mathrm{ZrPu}}$	$\tilde{D}_{\mathrm{PuZr}}$	$\tilde{D}_{\mathrm{PuPu}}$
0.16	–0.33	–0.10	1.7

In more detailed experiments, Dayananda, et al [10] obtained the interdiffusion coefficients for Ag-Zn-Cd at a number of different compositions, from which one could begin to develop a necessary functional dependence on composition. Note that in this system the cross coefficients are positive in contrast to the negative cross coefficients for U-Pu-Zr.

Diffusion behavior in ternary systems is substantially more complex than binary systems, particularly when multiple phases are involved (see [8]). Full phase diagram information is required, including a description of the tie lines through two-phase regions. The current model applies in a single phase.

The basic model (22) was implemented in Pedernal for testing, and is now being implemented in Bison. The Bison implementation is intended to serve as a starting point for further investigations of constituent migration in ternary systems.

Example

To illustrate the behavior of the model, we consider a problem in a cylindrical domain like the earlier problems. A uniform heat source is imposed that gives a center-to-outside temperature difference of 100 C. We use the interdiffusion coefficients for U-Pu-Zr given in the table, and arbitrarily choose $S_{Zr} = 0$ and $S_{Pu} = -10^{-7}$. Pedernal simulation results are shown in Figure 5. Starting from a uniform initial composition, the Pu is driven toward the center, up the temperature gradient, by its Soret term. The Zr, on the other hand is unaffected by the temperature gradient (its Soret coefficient is 0), but it too is driven toward the center by the cross diffusion term that couples it to the Pu gradient.

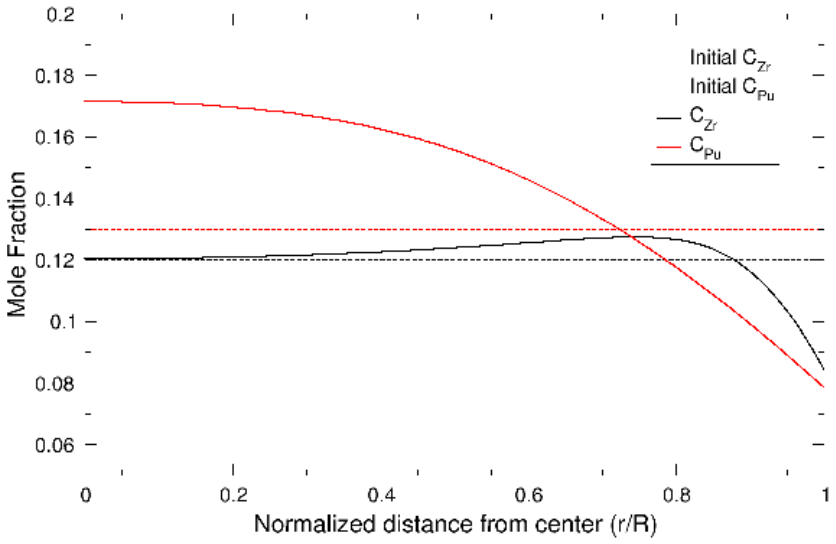

Figure 5: Ternary component migration

6. CONCLUSIONS

A computer model was developed to calculate constituent redistribution in U-Pu-Zr metallic fuel under irradiation within the MOOSE/BISON framework. This pseudo-binary model showed excellent agreement when compared to validation cases executed using the Pedernal code. A basic full ternary model was also developed and implemented. The modeling and simulation of constituent redistribution is an essential component of the simulation of fuel performance because the change in local composition affects the mechanical and thermal properties of the fuel as well as the radial power distribution. The creation and validation of a robust constituent redistribution model in BISON allows for continued development and refinement of additional pieces for furthering constituent redistribution work. Particularly this can allow for the coupling of thermal conductivity solutions with Zirconium dependencies, as well as heat

generation predictions based upon Zirconium concentrations. Further work based upon constituent dependent heat generation calculations may be aided by coupling the BISON constituent redistribution solver to neutronic codes for accurate heat generation calculations in an iterative process based upon the species distribution.

7. ACKNOWLEDGMENTS

We would like to thank Jason Hales, Richard Williamson, Pavel Medvedev, Derek Gaston, Steve Hayes, Jon Carmack and Richard Martineau for their help and support. We are very grateful to Kemal Pasamehmetoglu and DOE program manager Frank Goldner for their vision on the science based advanced fuel development program and the support they provided to develop the current analysis capability.

8. REFERENCES

[1]. Williamson RL, Hales JD, Novascone SR, Tonks MR, Gaston DR, Permann CJ, et al. Multidimensional multiphysics simulation of nuclear fuel behavior. Journal of Nuclear Materials. 2012 April; 423(1-3): p. 149-63.

[2] N.N. Carlson, "Final Report for Work Package LA0915090116: Fuel Performance Simulations," LA-UR-09-07340, (2009).

[3] G. L. Hofman et al., "Temperature Gradient Driven Constituent Redistribution in U-Zr Alloys," Journal of Nuclear Materials, Vol. 227, pp. 277-286, (1995).

[4] Y. S. Kim et al., "Modeling of Constituent Redistribution in U-Pu-Zr metallic Fuel," Journal of Nuclear Materials, Vol. 359, pp. 17-28, (2006).

[5] M. Ishida, T. Ogata, M. Kinoshita, Constituent Migration Model for U-Pu-Zr metallic fast reactor fuel, Nucl. Technol. 104 (1993).

[6] P.C. Shewmon, "The redistribution of a second phase during annealing in a temperature gradient", Trans. TMS-AIME 212 (1958).

[7] A.R. Allnatt, A.B. Lidiard, "Atomic Transport in Solids", Cambridge University Press, 1993.

[8] F.J.J. van Loo, Multiphase diffusion in binary and ternary solid-state systems. Prog. Solid St. Chem. Vol. 30 (1990).

[9] M.C. Petri, M.A. Dayananda, Isothermal diffusion in uranium-plutonium-zirconium alloys. J. Nucl. Mater. 240 (1997).

[10] P.T. Carlson, M.A. Dayananda, R.E. Grace, Diffusion in ternary Ag-Zn-Cd solid solutions. Metal. Trans. 3 (1972).

[11] C. Unal, N. Carlson, J. Galloway, "Preliminary Simulation Results of the Constituent Distribution Model Implemented into the BISON Framework for the Analysis of Performance of Metallic Fuels", International Conference on Fast Reactors and Related Fuel Cycles: Safe Technologies and Sustainable Scenarios (FR13), March 4-7 2013, Paris France.